

Article

Ab initio Investigation of the Thermochemistry and Kinetics of the $\text{SO}_2 + \text{O}_3^- \rightarrow \text{SO}_3^- + \text{O}_2$ Reaction in Aircraft Engines and the Environment

Xuechao Guo ^{1,2}, Alexey B. Nadykto ^{3,4}, Yisheng Xu ^{2,*}, Qingzhu Zhang ¹ and Jingtian Hu ^{1,*}

¹ Environment Research Institute, Shandong University, Jinan 250100, China;

E-Mails: sdgjy2012@163.com (X.G.); zqz@sdu.edu.cn (Q.Z.)

² State Key Laboratory of Environmental Criteria and Risk Assessment, Chinese Research Academy of Environmental Sciences, Beijing 100012, China

³ Atmospheric Science Research Center, State University of New York at Albany, 251 Fuller Road, Albany, NY 12203, USA; E-Mail: alexn@asrc.cestm.albany.edu

⁴ Department of Applied Mathematics, Moscow State Technological University “STANKIN”, Vadkovsky per., 1, Moscow, 127994, Russia

* Authors to whom correspondence should be addressed; E-Mails: xuys@craes.org.cn (Y.X.); hjt@sdu.edu.cn (J.H.); Tel.: +86-10-84915249 (Y.X.); Fax: +86-10-84915248 (Y.X.); +86-531-88366072 (J.H.).

External Editor: Kevin H. Knuth

Received: 30 September 2014; in revised form: 12 November 2014 / Accepted: 14 November 2014 /

Published: 1 December 2014

Abstract: In the present work, the mechanisms, thermochemistry and kinetics of the reaction of SO_2 with O_3^- have been studied using the CCSD(T)/6-31G(d) + CF method. It has been shown that there exist two possible pathways A and B of the $\text{SO}_2 + \text{O}_3^- \rightarrow \text{SO}_3^- + \text{O}_2$ reaction. The two pathways' A and B barrier heights are 0.61 kcal mol⁻¹ and 3.40 kcal mol⁻¹, respectively, while the energy of the $\text{SO}_2 + \text{O}_3^- \rightarrow \text{SO}_3^- + \text{O}_2$ reaction is -25.25 kcal mol⁻¹. The canonical variational transition state theory with small-curvature tunneling (CVT/SCT) has been applied to study the reaction kinetics. The CVT/SCT study shows that the rate constants K for pathways A and B, $K_A = 1.11 \times 10^{-12} \exp(-2526.13/T)$ and $K_B = 2.7 \times 10^{-14} \exp(-1029.25/T)$, respectively, grow as the temperature increases and are much larger than those of the $\text{SO}_2 + \text{O}_3 \rightarrow \text{SO}_3 + \text{O}_2$ reaction over the entire temperature range of 200–1500 K. This indicates that ionization of O_3 and high temperatures are favorable for the SO_2 oxidation via the reaction with ozone. The new data obtained in the present study can be utilized directly

for the evaluation of experiments and model predictions concerning SO₂ oxidation and kinetic modeling of gas-phase chemistry of pollutants/nucleation precursors formed in aircraft engines and the Earth's atmosphere.

Keywords: sulfur dioxide; ozone ion; atmospheric nucleation precursors; *ab initio*; density functional theory; rate constants

1. Introduction

Aerosols are critically important for the Earth's atmosphere [1–4]. They can be divided into two groups: primary and secondary aerosols. Primary aerosols are emitted directly into the Earth's atmosphere from various natural and anthropogenic sources, while secondary aerosols are formed via gas-phase nucleation [1–14]. Secondary aerosols strongly affect the entire atmospheric ecosystem [1–5]. Aerosols formed via the gas-phase nucleation play an important role in the aerosol radiative forcing and indirectly affect the Earth's climate by modifying cloud properties and precipitation [1–4]. They also impact the atmospheric micro- and macro-physics and chemistry, visibility, the Earth radiation budget [1–5,8–14] and public health [6,7]. New particles dominate the number concentration of atmospheric aerosols and their burst is frequently observed in the boundary layer and the lower troposphere [1–5].

Sulfuric acid is commonly accepted as a key species for atmospheric new particle formation because atmospheric vapours mixtures never nucleate before the H₂SO₄ concentration achieves the level of 10⁵ cm⁻¹ [1,3,4]. Binary H₂SO₄-H₂O nucleation (BHN) [5] adequately explain nucleation in the case when environment is clean [3]. However, it can not explain nucleation events observed in the more polluted areas [1–5]. This means that atmospheric nucleation is multicomponent, involves more than two species and can be described as a H₂SO₄-H₂O-X process. Sulfuric acid/ammonia clusters can be stabilized by organic acids [8–11] (e.g., maleic acid, oxalic acid and other dicarboxylic acids and possibly by large highly oxidized organics [2] such as, for example, C₁₀H₁₄O₇), bases such as amines and NH₃ [1–4,12–14] and ions [4,15]. It is important to note that while X is still a subject of ongoing debates, the H₂SO₄ is commonly accepted as the key atmospheric nucleation precursor [1–5].

H₂SO₄ is produced via chemical reactions involving e.g., neutral SO₂ and chemiions such as SO₃⁻, SO₄⁻, O₃⁻ and others of both biogenic and anthropogenic origin [3,5,16–20]. Sulfur dioxide is a precursor [16–20] to H₂SO₄, which is present in large concentrations in the Earth's atmosphere and produced in aircraft engines. Aircrafts generally produce significant amount of pollutants due to combustion of fossil fuel. Sulfur dioxides are the dominant product of the aviation kerosene combustion [21] and can be converted into the H₂SO₄ with the help of chemiions generated in engines [21–23]. While ozone is one of the most important contributors to the oxidation of SO₂ to sulfates in clouds [16–29], negatively charged O₃⁻ is a common chemiion generated in engines [21–23] and produced via the charge-transfer reactions and particle transfer reactions in Earth's atmosphere [24–26].

The SO₂ conversion into sulfuric acid in the Earth's atmosphere includes two stages [16,24–42]. The first stage is the sulfur dioxide oxidation to sulfur trioxide [16,24–36]. The second stage is the sulfur trioxide hydrolysis to sulfuric acid [37–42]. The conversion of SO₂ into SO₃ and H₂SO₄ has been investigated using experimental and theoretical methods in the past [16,24–36]. For example, the

reviews of experiments relevant to the gas-phase conversion SO_2 into the sulfuric acid has been presented in [16,30]. Starik with co-workers have investigated the concentrations of sulfate aerosol precursors and chemiions in the aircraft engines using advanced numerical models [34]. Ozone injection methods used to simultaneously remove NO_x and SO_2 in the flue gas have been investigated by Mok and Lee [35,36]. Davis with co-workers [32] have employed stop-flow time-of-flight mass spectrometry to study the reaction of SO_2 and O_3 and obtained the rate constant of $2 \times 10^{-22} \text{ cm}^3 \text{ molecule}^{-1} \text{ s}^{-1}$ at 300 K for $\text{SO}_2 + \text{O}_3 \rightarrow \text{SO}_3 + \text{O}_2$ reaction. More recently, Jiang *et al.* [43] have carried out a quantum chemical study and obtained a value of $3.61 \times 10^{-23} \text{ cm}^3 \text{ molecule}^{-1} \text{ s}^{-1}$ at 300 K for the same reaction. However, although the SO_2 oxidation has been studied in the past, a deep and insightful understanding of the mechanisms, thermochemistry and kinetics of the SO_2 oxidation via the reaction with ozone, including the impact of O_3 charging on the reaction mechanisms and reaction rate, are yet to be achieved. In particular, the mechanism of the the $\text{SO}_2 + \text{O}_3^- \rightarrow \text{SO}_3^- + \text{O}_2$ reaction, which occurs in aircraft engines and environment, is poorly understood. Currently, no data on the thermochemistry and kinetics of the $\text{SO}_2 + \text{O}_3^- \rightarrow \text{SO}_3^- + \text{O}_2$ reaction are available

In order to fill this gap and to achieve a deeper and more insightful understanding of mechanisms of SO_2 oxidation, we have carried out the *ab initio* study of reactions of SO_2 , the precursor to gaseous H_2SO , with the common chemiion O_3^- and have investigated the reaction mechanisms, thermochemistry and kinetics. The new data that characterize the above-mentioned properties and can be utilized directly for the assessment of the efficiency of different SO_2 oxidation mechanisms and kinetic modeling of gas-phase chemistry of pollutants/nucleation precursors have been obtained. The comparison of the newly obtained data with the data for $\text{SO}_2 + \text{O}_3 \rightarrow \text{SO}_3 + \text{O}_2$ reaction has been carried out and the impact of the O_3 ionization and temperature on the reaction thermochemistry and kinetics has been discussed.

2. Methods

The computations have been carried out using the Gaussian 03 suite of programs [44] using the CCSD(T)/6-31G(d) + CF method. The method employed in the present study has been widely used to compute the reaction energies and to investigate reactions involving atmospheric species [45–53].

In the framework of the CCSD(T)/6-31G(d) + CF method, the geometries of all the reactants, transition states, complexes and products were optimized at the B3LYP/aug-cc-pvdz level of theory. The vibrational spectra have been calculated in order to determine the nature of stationary points. Stationary points were classified as minima in the case, when no imaginary frequencies were present in the vibrational spectrum, while those with one imaginary frequency in the spectrum are identified as transitional states [51]. Each transitional state has been examined using the intrinsic reaction coordinate (IRC) method [54] at the B3LYP/aug-cc-pvdz level in order to make sure that the transition states properly connect reactants and products. Zero-point energies (ZPE) have also been calculated using the B3LYP/aug-cc-pvdz. B3LYP/aug-cc-pvdz optimized geometries were used for the single-point energy calculations with B3LYP and high-level Coupled-Cluster method with Single and Double excitations including perturbative corrections for the Triple excitations (CCSD(T)). In order to achieve high accuracy in computed single-point energies, the basis set effects were corrected [52]. A correction factor (CF) was derived from the energy difference between the B3LYP/6-31G(d) and B3LYP/6-311++G(3df,2pd) levels of theory. Energies calculated using the CCSD(T)/6-31G(d) were then corrected by the CF.

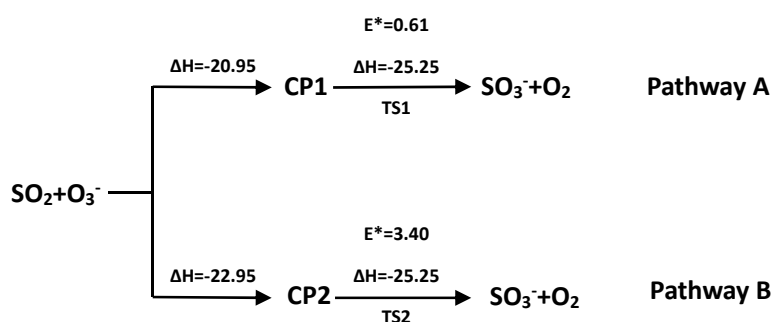
In order to ensure the quality of the obtained results, additional calculations with MP2, CCSD(T) and QCISD(T) methods with different basis sets have been carried out. The reaction rate constants have been calculated with the canonical variational transition state theory (CVT) with small-curvature tunneling (SCT) effect [55,56] using the optimized geometries, energy and Hessian data of all the reactants, complexes, transition states and products. The rate calculations were carried out using Polyrate 9.7 Suite of Programs [57].

3. Result and Discussion

3.1. Reaction Mechanism

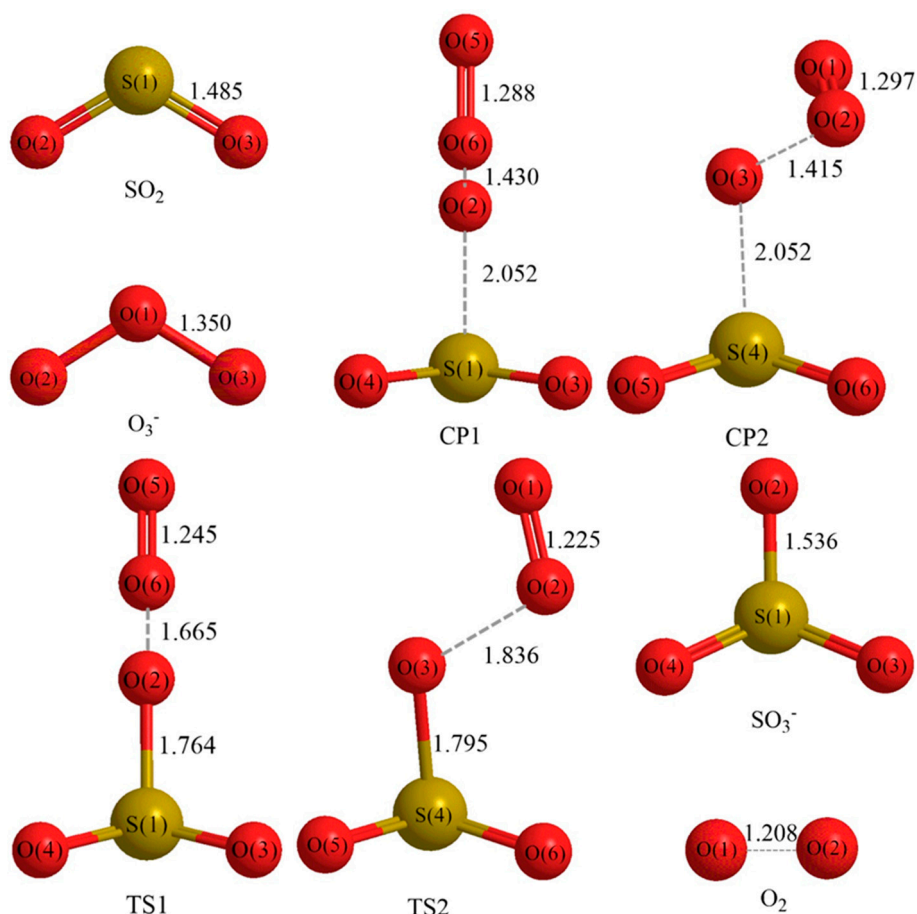
Sulfur dioxide molecule attacks negatively charged ozone ion, captures the oxygen atom from O_3^- and subsequently forms negatively charged sulfur trioxide ion and oxygen molecule [35]. Sulfur dioxide molecules can approach negatively charged ozone ion in two ways corresponding to two possible reaction pathways. The possible reaction pathways are shown in Scheme 1. Figure 1 presents the optimized geometries of the reactants, complexes, transition states and products and the most important geometrical properties characterizing these systems.

Scheme 1. The possible reaction pathways of the $\text{SO}_2 + \text{O}_3^- \rightarrow \text{SO}_3^- + \text{O}_2$ reaction with the potential barriers E^* (kcal mol^{-1}) and reaction heats (kcal mol^{-1}).



Two transition states (TS1 and TS2) have been identified. Both transition states have only one imaginary harmonic vibrational frequency and can be classified as the first-order saddle points. The values of the imaginary frequencies for TS1 and TS2 transition states are $-528.1303i$ and $-436.9066i$, respectively. In order to ensure that the transition states connect corresponding reactants and products, the intrinsic reaction coordinate (IRC) calculations have been performed. The calculations of the relative energies of transition states indicate that van der Waals complexes CP1 and CP2 were formed prior to the formation of corresponding transition states.

Figure 1. Geometries of stationary points associated with the $\text{SO}_2 + \text{O}_3^- \rightarrow \text{SO}_3^- + \text{O}_2$ reaction obtained at B3LYP/aug-cc-pvdz level of theory. Bond distances are given in Å. TS1 and TS2 denote transition states of pathway A and B, respectively.



In the case of the pathway A, the sulfur dioxide molecule approaches the ozone ion vertically and captures the terminal oxygen atom. The barrier height of the pathway A is $0.61 \text{ kcal mol}^{-1}$. CP1 was formed prior to TS1. The O(2)-O(6) bond is 0.080 \AA longer than O-O bonds in O_3^- molecule, while O(5)-O(6) bond reduced in length to 1.288 \AA . The S(1)-O(2) was found to be 2.052 \AA . As the reaction continued, the TS1 was formed. S(1)-O(2) bond length of 1.764 \AA in TS1 is 0.288 \AA shorter than S(1)-O(2) in CP1. O(5)-O(6) bond reduced in lengths to 1.245 \AA and is now close to the double O-O bond (1.208 \AA). The length of O(2)-O(6) is 1.665 \AA that is 0.235 \AA longer than the corresponding bond in CP1. The lengths of the S(1)-O(2) bond in SO_3^- is 1.536 \AA that is 0.228 \AA shorter than the corresponding bond in TS1. The double 1.208 \AA O(1)-O(2) bond was formed in the oxygen molecule.

In case of pathway B, sulfur dioxide molecule approaches the negative ozone ion slantly and captures the terminal oxygen atom. The barrier height of the pathway B is $3.40 \text{ kcal mol}^{-1}$. CP2 is formed prior to the formation of TS2. The S(4)-O(3) (2.052 \AA) in CP2 is nearly identical to the S(1)-O(2) (2.052 \AA) in CP1. The S(4)-O(3) bond in TS2 is 1.795 \AA that is 0.257 \AA shorter than the corresponding bond in CP2. The lengths of O(1)-O(2) bond in the TS2 is 1.225 \AA that is 0.072 \AA and 0.125 \AA shorter than the O-O bonds in CP2 and O_3^- , respectively, and close to the lengths of the double O-O bond of O_2 .

3.2. Thermochemical Analysis

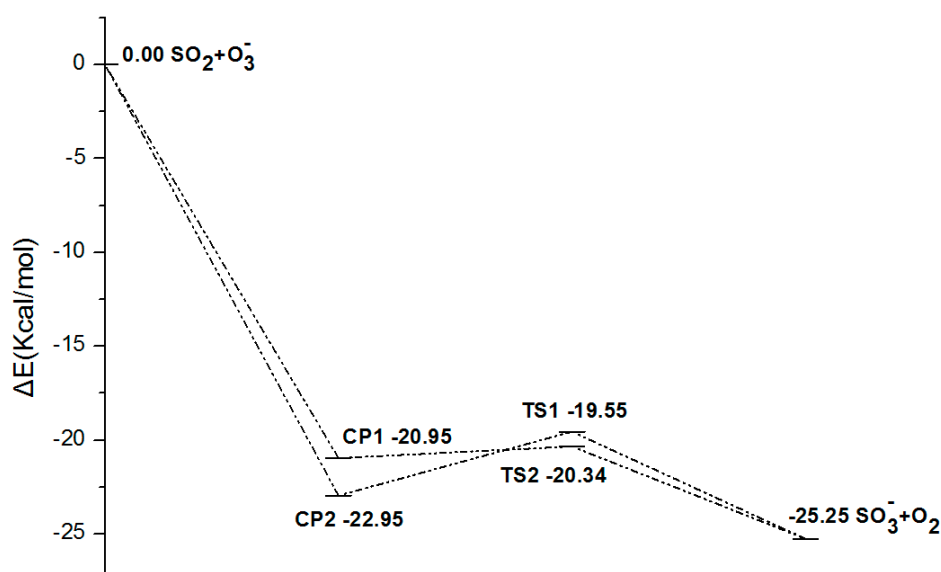
The $\text{SO}_2\text{-O}_3^-$ reaction energies for pathways A and B calculated using different methods are presented in Table 1. As it may be seen from Table 1, the reaction energies calculated using *ab initio* or *ab initio*-based methods are quite close, while those obtained by B3LYP/6-31G(d) and B3LYP/6-311++G(3df,2pd) methods significantly differ from the *ab initio* results. The RE values obtained at MP2/6-31G(d), CCSD(T)/6-31G(d), CCSD(T)/6-31G(d) + CF levels of theory agree within less than 3 kcal mol⁻¹, while the B3LYP/6-31G(d) and B3LYP/6-311++G(3df,2pd) predictions deviate from *ab initio* results by 6–10 kcal mol⁻¹. At the CCSD(T)/6-31G(d) + CF level of theory, the products are predicted to be -25.25 kcal mol⁻¹ more stable than the reactants. Figure 2 presents the profile of the potential energy surface for sulfur dioxide and negatively charged ozone ion calculated at the CCSD(T)/6-31G(d) + CF level of theory.

Table 1. Comparison of the $\text{SO}_2 + \text{O}_3^- \rightarrow \text{SO}_3^- + \text{O}_2$ reaction energies (RE), the relative energies of the van der Waals complexes with respect to reactants (RE_{cp}) and potential energy barriers (ΔE) with zero-point correction included (kcal mol⁻¹) for the pathways A and B calculated at different levels of theory in the present study with and energies of the $\text{SO}_2 + \text{O}_3 \rightarrow \text{SO}_3 + \text{O}_2$ reaction [43].

Method	RE_{cp1}	RE_{cp2}	ΔE_1	ΔE_2	RE
MP2/6-31G(d)	-24.64	-26.23	2.66	10.17	-28.90
B3LYP/6-31G(d)	-36.38	-37.33	1.48	12.17	-18.65
B3LYP/6-311++G(3df,2pd)	-26.59	-28.25	1.37	11.71	-17.77
CCSD(T)/6-31G(d)	-30.75	-32.03	0.72	3.86	-26.13
CCSD(T)/6-31G(d)+CF	-20.95	-22.95	0.61	3.40	-25.25
G2M ^a	-	-	9.68	-	-27.45

^a $\text{SO}_2 + \text{O}_3 \rightarrow \text{SO}_3 + \text{O}_2$ reaction [43].

Figure 2. The potential energy surface for the $\text{SO}_2 + \text{O}_3 \rightarrow \text{SO}_3^- + \text{O}_2$ reaction.



As seen from Table 1, the potential energy barriers with zero-point correction included for Pathway A and B are quite sensitive to the basis sets even if a DFT method such as B3LYP is applied. In order to correct the basis set effect, we have employed the basis set correction method [52]. The potential energy barriers predicted at the CCSD(T)/6-31G(d) + CF level of theory for pathways A and B were found to be 0.61 kcal mol⁻¹ and 3.40 kcal mol⁻¹, respectively. As it may be seen from Table 1, potential energy barriers for pathways A and B differ by less than 2.7 kcal mol⁻¹.

The relative energies of transition states of both pathways computed at all the MP2, B3LYP and CCSD(T) levels of theory are negative. This is a clear indication of the formation of complexes prior to the formation of the transition state. The relative energies for CP1 and CP2 with zero-point corrections included are shown in Table 1. The CCSD(T)/6-31+G(d) + CF values for CP1 and CP2 are -20.95 kcal mol⁻¹ and -22.95 kcal mol⁻¹ respectively. The values are more negative than energies of the corresponding transition states, -20.34 kcal mol⁻¹ and -19.55 kcal mol⁻¹, respectively. This is a clear indication of the possible formation of associated complexes prior to the formation of the corresponding transition states.

As it may be seen in Table 1, the SO₂ + O₃ → SO₃ + O₂ reaction energy [43] is close to that the energy of the SO₂ + O₃⁻ → SO₃⁻ + O₂ obtained in the present study. However, the barrier of the SO₂ + O₃ → SO₃ + O₂ reaction is by 9 kcal mol⁻¹ higher than that of SO₂ + O₃⁻ → SO₃⁻ + O₂ reaction. This shows clearly that the O₃ charging greatly reduces the barrier of the reaction of SO₂ with ozone.

In order to ensure the quality of the obtained results, we have performed additional high levels ab initio calculations using CCSD(T)/6-311G(d,p) and QCISD(T)/6-311G(d,p) methods. The results of these calculations are summarized in Table 2. As it may be seen from Table 2, the activation energies obtained at CCSD(T)/6-31G(d) + CF and CCSD(T)/6-311G(d,p) levels of theory are very close, with the largest difference of 1.8 kcal mol⁻¹ only. Activation energies produced by the CCSD(T)/6-31G(d) + CF and QCISD(T)/6-311G(d,p) methods are also in agreement within 1.69 kcal mol⁻¹ and 0.97 kcal mol⁻¹ in the case of pathways A and B, respectively. This means that CCSD(T)/6-31G(d) + CF method adequately describes the reaction energies and that CCSD(T)/6-31G(d) + CF data can readily be used for kinetic calculations of rate constants.

Table 2. Activation energies (kcal mol⁻¹) for the abstraction reaction of sulfur dioxide with negatively charged ozone molecule calculated using high level ab *initio* methods.

Pathway	CCSD(T)/ 6-31G(d)	CCSD(T)/ 6-31G(d)+CF	CCSD(T)/ 6-311G(d,p)	QCISD(T)/ 6-311G(d,p)
A	0.72	0.61	2.41	2.30
B	3.86	3.40	2.53	4.37

3.3. Reaction Kinetics

The CVT/SCT method was used for the kinetic calculations. Since the temperature in aircraft engines decreases from 1500 K near the combustor to 600 K near the nozzle, the temperature range of 200–1500 K has been chosen for kinetic calculations to represent both aircraft engine and atmospheric conditions.

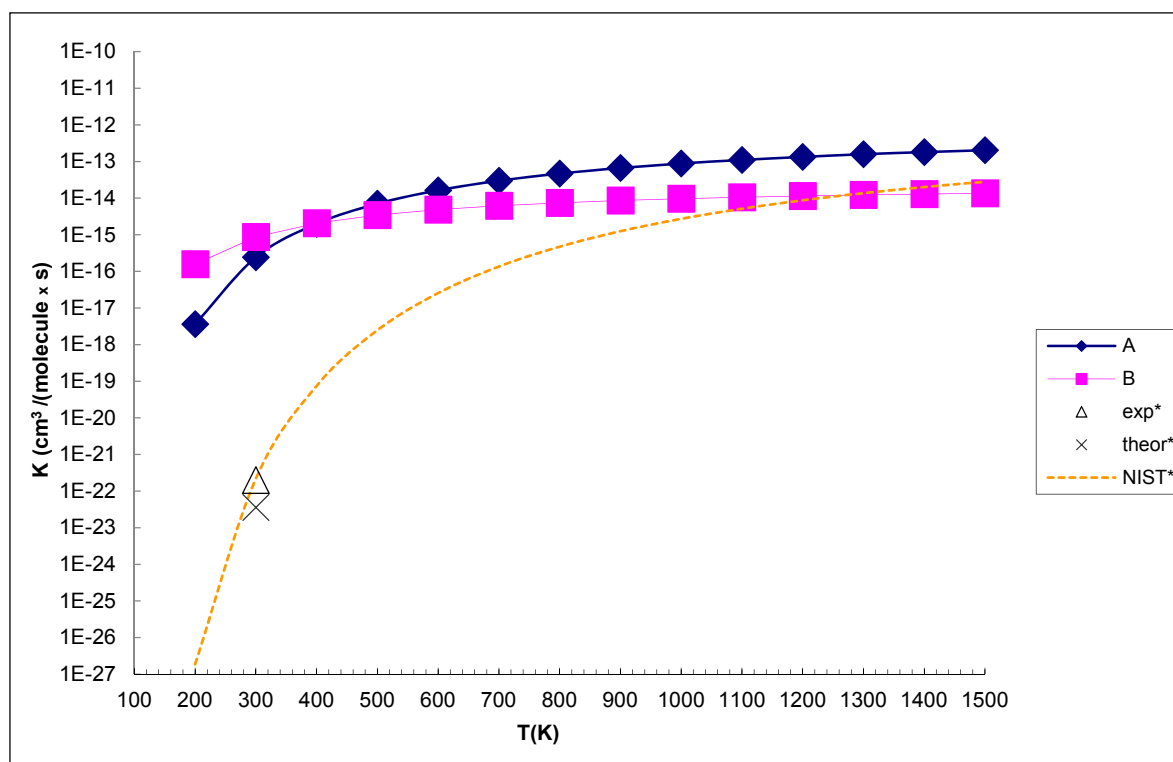
The CVT/SCT rate constants calculated at 200–1500 K with the input parameters obtained at the CCSD(T)/6-31G(d) + CF level of theory are shown in Table 3. The rate constants for pathways A and B were fitted using the Arrhenius formula to obtain $K_A = 1.11 \times 10^{-12} \exp(-2526.13/T)$ and

$k_B = 2.7 \times 10^{-14} \exp(-1029.25/T)$ respectively. Figure 3 shows the comparison of k_A and k_B with the rate constants for the $\text{SO}_2 + \text{O}_3 \rightarrow \text{SO}_3 + \text{O}_2$ reaction by Davis *et al.* [32], Jiang *et al.* [43] and NIST data [58].

Table 3. Rate constants k_A and k_B at 200–1500 K.

T(K)	Pathway A ($\text{cm}^3 \text{mol}^{-1} \text{s}^{-1}$)	Pathway B ($\text{cm}^3 \text{mol}^{-1} \text{s}^{-1}$)
200	3.63×10^{-18}	1.57×10^{-16}
300	2.45×10^{-16}	8.74×10^{-16}
400	2.07×10^{-15}	2.06×10^{-15}
500	7.60×10^{-15}	3.45×10^{-15}
600	2.04×10^{-14}	5.51×10^{-15}
700	2.98×10^{-14}	6.21×10^{-15}
800	4.21×10^{-14}	6.99×10^{-15}
900	5.78×10^{-14}	7.85×10^{-15}
1000	7.74×10^{-14}	8.81×10^{-15}
1100	1.01×10^{-13}	9.89×10^{-15}
1200	1.30×10^{-13}	1.11×10^{-14}
1300	1.65×10^{-13}	1.24×10^{-14}
1400	2.05×10^{-13}	1.39×10^{-14}
1500	2.52×10^{-13}	1.56×10^{-14}

Figure 3. Comparison of the rate constants k_A and k_B for $\text{SO}_2 + \text{O}_3^- \rightarrow \text{SO}_3^- + \text{O}_2$ reaction at 200–1500 K with the experimental and theoretical data for the $\text{SO}_2 + \text{O}_3 \rightarrow \text{SO}_3 + \text{O}_2$ reaction [32,43,58]. Symbols A, B, exp*, theor*, NIST* refer to pathway A (present study), pathway B (present study), ref. [32], ref. [43] and NIST fitted data ref. [58], respectively.



As it can be seen from Table 3, the rate constants for both pathways grow with the temperature over the full range of temperatures. The rate constants for pathways A and B are very close and differ by a factor of 2–10 only. As it may be seen from Table 3 and Figure 3, at temperatures typical for inside of aircraft engines, the pathway A dominates over pathway B and that the high temperature zones, which are located near the combustor, are the sites, where most of the SO₂-to-SO₃⁻ conversion occurs. In contrast, at the atmospheric temperatures the pathway B dominates over the pathway A. The rate constants at 300 K are $2.45 \times 10^{-16} \text{ cm}^3 \text{ molecule}^{-1} \text{ s}^{-1}$ and $8.74 \times 10^{-16} \text{ cm}^3 \text{ molecule}^{-1} \text{ s}^{-1}$ for pathway A and pathway B, respectively. The rate constants for the SO₂ + O₃⁻ → SO₃⁻ + O₂ reaction appear to be much larger than those obtained by Davis *et al.* [32] ($2 \times 10^{-22} \text{ cm}^3 \text{ molecule}^{-1} \text{ s}^{-1}$ at T = 300 K) and Jiang *et al.* [43] ($3.61 \times 10^{-23} \text{ cm}^3 \text{ molecule}^{-1} \text{ s}^{-1}$ at T = 300 K) for SO₂ + O₃ → SO₃ + O₂ reaction. The rate constants for SO₂ + O₃⁻ → SO₃⁻ + O₂ reaction (either A, or both A and B) are much larger than the rate constants for SO₂ + O₃ → SO₃ + O₂ reaction over the whole temperature range of 200–1500 K. These considerations lead us to the conclusion that high temperatures and negative charging of ozone are favorable for the SO₂ oxidation via the reaction with ozone.

4. Conclusions

In this study, the mechanisms of the oxidation of SO₂, precursor to H₂SO₄, via the reaction with negatively charged ozone molecules, the common chemiion generated in engines and produced via the charge-transfer reactions and particle transfer reactions in Earth's atmosphere, have been investigated using the CCSD(T)/6-31G(d) + CF method. The present study leads us to the following conclusions:

- (1) There exist two pathways of the SO₂ + O₃⁻ → SO₃⁻ + O₂ reaction, pathway A and pathway B. The reaction energy is $-25.25 \text{ kcal mol}^{-1}$, while the activation energies for pathways A and B are $0.61 \text{ kcal mol}^{-1}$ and $3.40 \text{ kcal mol}^{-1}$, respectively. It is also important to note that while *ab initio* and *ab initio*-based methods predict the reaction energy in very good agreement with each other, both B3LYP/6-31G(d) and B3LYP/6-311++G(3df,2pd) underestimate the reaction energy by 6–10 kcal mol⁻¹.
- (2) The analysis of the reaction kinetics shows clearly that while the rate constants for pathways A and B, $K_A = 1.11 \times 10^{-12} \exp(-2526.13/T)$ and $K_B = 2.7 \times 10^{-14} \exp(-1029.25/T)$, differ by a factor of 2–10 only, pathway A dominates over the pathway B over the whole range of temperatures typical for aircraft engines (600–1500 K). However, at lower temperatures typical for the Earth's atmosphere the pathway B dominates over the pathway A.
- (3) The rate constants for both pathway A and pathway B grow with the temperature. This means that the high temperature zones, which are located near the combustor, are the sites, where most of the SO₂ to SO₃⁻ conversion in the aircraft engines occurs.
- (4) The SO₂ + O₃ → SO₃ + O₂ reaction energy [34] is close to that the energy of the SO₂ + O₃⁻ → SO₃⁻ + O₂ obtained in the present study. However, the barrier of the SO₂ + O₃ → SO₃ + O₂ reaction is by 9 kcal mol⁻¹ higher than that of SO₂ + O₃⁻ → SO₃⁻ + O₂ reaction. This shows clearly that the O₃ charging greatly reduces the barrier of the reaction of SO₂ with ozone. The rate constants for the SO₂ + O₃⁻ → SO₃⁻ + O₂ reaction at atmosphere temperatures are much larger than those obtained by Davis *et al.* [32] ($2 \times 10^{-22} \text{ cm}^3 \text{ molecule}^{-1} \text{ s}^{-1}$ at T = 300 K) and Jiang *et al.* [43] ($3.61 \times 10^{-23} \text{ cm}^3 \text{ molecule}^{-1} \text{ s}^{-1}$ at T = 300 K) for the SO₂ + O₃ → SO₃ + O₂ reaction.

These considerations lead us to conclude that both high temperatures and charging are favorable for the SO₂ oxidation via the reaction with ozone. This finding has important implications for the physics and chemistry of atmospheric pollutants formed in aircraft engines and the Earth's atmosphere, while new data obtained in the present study can be utilized directly for the evaluation of experiments and model predictions concerning SO₂ oxidation and kinetic modeling of gas-phase chemistry of gaseous pollutants and nucleation precursors.

Acknowledgments

This work was supported by the National Natural Science Foundation of China (Grant 41375133) and the Science Foundation of Chinese Research Academy of Environmental Sciences (Grant 2012-YSKY-15). Additional support was provided by the CRAES Supercomputing Facilities (SGI 4700 super computers). ABN also thanks the Russian Ministry of Education and Science for support under the Federal Research Program.

Author Contributions

Yisheng Xu, Jingtian Hu and Xuechao Guo conceived and designed the research; Xuechao Guo, Alexey B. Nadykto and Yisheng Xu performed the calculations and analyzed the data; Xuechao Guo, Yisheng Xu and Jingtian Hu contributed to the writing of the manuscript; Alexey B. Nadykto polished and reviewed the English writing in advance; Qingzhu Zhang provided the POLYRATE 9.7 suite of program and gave advices on kinetics calculation. All authors have read and approved the final manuscript.

Conflicts of Interest

The authors declare no conflict of interest.

References

1. Zhang, R. Getting to the critical nucleus of aerosol formation. *Science* **2010**, *328*, 1366–1367.
2. Almeida, J.; Schobesberger, S.; Kürten, A.; Ortega, I.K.; Kupiainen-Määttä, O.; Praplan, A.P.; Adamov, A.; Amorim, A.; Bianchi, F.; Breitenlechner, M.; *et al.* Molecular understanding of sulphuric acid-amine particle nucleation in the atmosphere. *Nature* **2013**, *502*, 359–363.
3. Zhang, R.; Khalizov, A.F.; Wang, L.; Hu, M.; Wen, X. Nucleation and growth of nanoparticles in the atmosphere. *Chem. Rev.* **2012**, *112*, 1957–2011.
4. Yu, F.; Luo, G. Simulation of particle size distribution with a global aerosol model: Contribution of nucleation to aerosol and CCN number concentrations. *Atmos. Chem. Phys.* **2009**, *9*, 7691–7710.
5. Sipila, M.; Berndt, T.; Petaja, T.; Brus, D.; Vanhanen, J.; Stramann, F.; Patokoski, J.; Mauldin, R.L., III; Hyvarinen, A.-P.; Lihavainen, H.; *et al.* The role of sulfuric acid in atmospheric nucleation. *Science* **2010**, *327*, 1243–1246.
6. Knaapen, A.M.; Borm, P.J.; Albrecht, C.; Schins, R.P. Inhaled particles and lung cancer. Part A: Mechanisms. *Int. J. Cancer* **2004**, *109*, 799–809.
7. Saxon, A.; Diaz-Sanchez, D. Air pollution and allergy: You are what you breathe. *Nature Immunol.* **2005**, *6*, 223–226.

8. Zhang, R.; Suh, I.; Zhao, J.; Zhang, D.; Fortner, E.C.; Tie, X.; Molina, L.T.; Molina, M.J. Atmospheric new particle formation enhanced by organic acids. *Science* **2004**, *304*, 1487–1490.
9. Xu, Y.; Nadykto, A.B.; Yu, F.; Jiang, L.; Wang, W. Formation and properties of hydrogen-bonded complexes of common organic oxalic acid with atmospheric nucleation precursors. *J. Mol. Struct.* **2010**, *951*, 28–33.
10. Xu, W.; Zhang, R. A theoretical study of hydrated molecular clusters of amines and dicarboxylic acids. *J. Chem. Phys.* **2013**, *139*, doi:10.1063/1.4817497.
11. Xu, Y.; Nadykto, A.B.; Yu, F.; Herb, J.; Wang, W. Interaction between common organic acids and trace nucleation species in the earth's atmosphere. *J. Phys. Chem. A* **2009**, *114*, 387–396.
12. Kurten, T.; Loukonen, V.; Vehkamäki, H.; Kulmala, M. Amines are likely to enhance neutral and ion-induced sulfuric acid-water nucleation in the atmosphere more effectively than ammonia. *Atmos. Chem. Phys.* **2008**, *8*, 4095–4103.
13. Nadykto, A.B.; Yu, F.; Yakovleva, M.; Herb, J.; Xu, Y. Amines in the earth's atmosphere: A DFT study of the thermochemistry of pre-nucleation clusters. *Entropy* **2011**, *13*, 554–569.
14. Nadykto, A.B.; Herb, J.; Yu, F.; Xu, Y. Enhancement in the production of nucleating clusters due to dimethylamine and large uncertainties in the thermochemistry of amine-enhanced nucleation. *Chem. Phys. Lett.* **2014**, *609*, 42–19.
15. Yu, F.; Turco, R.P. From molecular clusters to nanoparticles: The role of ambient ionization in tropospheric aerosol formation. *J. Geophys. Res.* **2001**, *106*, 4797–4814.
16. Laaksonen, A.; Pirjola, L.; Kulmala, M.; Wohlfrom, K.-H.; Arnold, F.; Raes, F. Upper tropospheric SO₂ conversion into sulfuric acid aerosols and cloud condensation nuclei. *J. Geophys. Res. Atmos.* **2000**, *105*, 1459–1469.
17. Liao, H.; Zhang, Y.; Chen, W.-T.; Raes, F.; Seinfeld, J.H. Effect of chemistry-aerosol-climate coupling on predictions of future climate and future levels of tropospheric ozone and aerosols. *J. Geophys. Res.* **2009**, *114*, doi:10.1029/2008JD010984.
18. Rowland, F.S. Stratospheric ozone depletion. *Phil. Trans. R. Soc. Lond. B* **2006**, *361*, 769–790.
19. Fenger, J. Air pollution in the last 50 years—From local to global. *Atmos. Environ.* **2009**, *43*, 13–22.
20. Lelieveld, J.; Butler, T.M.; Crowley, J.N.; Dillon, T.J.; Fischer, H.; Ganzeveld, L.; Harder, H.; Lawrence, M.G.; Martinez, M.; Taraborrelli, D.; Williams, J. Atmospheric oxidation capacity sustained by a tropical forest. *Nature* **2008**, *452*, 737–740.
21. Brown, R.C.; Anderson, M.R.; Miake-Lye, R.C.; Kolb, C.E.; Sorokin, A.A.; Buriko, Y.Y. Aircraft exhaust sulfur emissions. *Geophys. Res. Lett.* **1996**, *23*, 3603–3606.
22. Fialkov, A.B. Investigations on ions in flames. *Prog. Energy Combust. Sci.* **1997**, *23*, 399–528.
23. Lifshitz, C.; Wu, R.; Tiernan, T.; Terwilliger, D. Negative ion-molecule reactions of ozone and their implications on the thermochemistry of O₃⁻. *J. Chem. Phys.* **1978**, *68*, 247–260.
24. Fehsenfeld, F.; Schmeltekopf, A.; Schiff, H.; Ferguson, E. Laboratory measurements of negative ion reactions of atmospheric interest. *Planet. Space Sci.* **1967**, *15*, 373–379.
25. Maahs, H.G. Measurements of the oxidation rate of sulfur (IV) by ozone in aqueous solution and their relevance to SO₂ conversion in nonurban tropospheric clouds. *Atmos. Environ. (1967)* **1983**, *17*, 341–345.
26. Möller, D. Kinetic model of atmospheric SO₂ oxidation based on published data. *Atmos. Environ. (1967)* **1980**, *14*, 1067–1076.

27. Bork, N.; Loukonen, V.; Vehkamäki, H. Reactions and reaction rate of atmospheric SO₂ and O₃⁻(H₂O)_n collisions via molecular dynamics simulations. *J. Phys. Chem. A* **2013**, *117*, 143–3148.
28. Bork, N.; Kurtén, T.; Enghoff, M.B.; Pedersen, J.O.P.; Mikkelsen, K.V.; Svensmark, H. Structures and reaction rates of the gaseous oxidation of SO₂ by an O₃⁻(H₂O)₀₋₅ cluster—A density functional theory investigation. *Atmos. Chem. Phys.* **2012**, *12*, 3639–3652.
29. Bork, N.; Kurtén, T.; Vehkamäki, H. Exploring the atmospheric chemistry of O₂SO₃⁻; and assessing the maximum turnover number of ion-catalysed H₂SO₄ formation. *Atmos. Chem. Phys.* **2013**, *13*, 3695–3703.
30. Hoffmann, M.R. On the kinetics and mechanism of oxidation of aquated sulfur dioxide by ozone. *Atmos. Environ. (1967)* **1986**, *20*, 1145–1154.
31. Mok, Y.S.; Lee, H.-J. Removal of sulfur dioxide and nitrogen oxides by using ozone injection and absorption-reduction technique. *Fuel Process. Technol.* **2006**, *87*, 591–597.
32. Davis, D.; Prusaczyk, J.; Dwyer, M.; Kim, P. Stop-flow time-of-flight mass spectrometry kinetics study. Reaction of ozone with nitrogen dioxide and sulfur dioxide. *J. Phys. Chem.* **1974**, *78*, 1775–1779.
33. Schumann, U.; Arnold, F.; Busen, R.; Curtius, J.; Kärcher, B.; Kiendler, A.; Petzold, A.; Schlager, H.; Schröder, F.; Wohlfrom, K.H. Influence of fuel sulfur on the composition of aircraft exhaust plumes: The experiments SULFUR 1–7. *J. Geophys. Res. Atmos. (1984–2012)* **2002**, *107*, 1–27.
34. Starik, A.M.; Savel'ev, A.M.; Titova, N.S.; Schumann, U. Modeling of sulfur gases and chemiions in aircraft engines. *Aerosp. Sci. Technol.* **2002**, *6*, 63–81.
35. Ferguson, E.E. Negative ion-molecule reactions. *Can. J. Chem.* **1969**, *47*, 1815–1820.
36. Mok, Y.S.; Lee, H.-J. Removal of sulfur dioxide and nitrogen oxides by using ozone injection and absorption-reduction technique. *Fuel Process. Technol.* **2006**, *87*, 591–597.
37. Torrent-Sucarrat, M.; Francisco, J.S.; Anglada, J.M. Sulfuric acid as autocatalyst in the formation of sulfuric acid. *J. Am. Chem. Soc.* **2012**, *134*, 20632–20644.
38. Morokuma, K.; Muguruma, C. Ab *initio* molecular orbital study of the mechanism of the gas phase reaction SO₃ + H₂O: Importance of the second water molecule. *J. Am. Chem. Soc.* **1994**, *116*, 10316–10317.
39. Long, B.; Chang, C.R.; Long, Z.W.; Wang, Y.B.; Tan, X.F.; Zhang, W.J. Nitric acid catalyzed hydrolysis of SO₃ in the formation of sulfuric acid: A theoretical study. *Chem. Phys. Lett.* **2013**, *581*, 26–29.
40. Gonzalez, J.; Torrent-Sucarrat, M.; Anglada, J.M. The reactions of SO₃ with HO₂ radical and H₂O...HO₂ radical complex. Theoretical study on the atmospheric formation of HSO₅ and H₂SO₄. *Phys. Chem. Chem. Phys.* **2010**, *12*, 2116–2125.
41. Hazra, M.K.; Sinha, A. Formic acid catalyzed hydrolysis of SO₃ in the gas phase: A barrierless mechanism for sulfuric acid production of potential atmospheric importance. *J. Am. Chem. Soc.* **2011**, *133*, 17444–17453.
42. Long, B.; Long, Z.W.; Wang, Y.B.; Tan, X.F.; Han, Y.; Long, C.; Qin, S.; Zhang, W. Formic acid catalyzed the gas phase reaction of H₂O with SO₃ and its reverse reaction: A theoretical study. *Phys. Chem.* **2012**, *13*, 323–329
43. Jiang, S.-D.; Wang, Z.-H.; Zhou, J.-H.; Wen, Z.-C.; Cen, K.-F. A quantum chemistry study on reaction mechanisms of SO₂ with O₃ and H₂O₂. *J. Zhejiang Univ. Sci. A* **2009**, *10*, 1327–1333.
44. Frisch, M.; Trucks, G.; Schlegel, H.; Scuseria, G.; Robb, M.; Cheeseman, J.; Montgomery, J., Jr;

- Vreven, T.; Kudin, K.; Burant, J. *Gaussian 03, Revision E. 01*; Gaussian Inc.: Wallingford, CT, USA, 2004.
45. Zhao, J.; Zhang, R. A theoretical investigation of nitrooxyalkyl peroxy radicals from NO₃-initiated oxidation of isoprene. *Atmos. Environ.* **2008**, *42*, 5849–5858.
46. Suh, I.; Zhao, J.; Zhang, R. Unimolecular ring-cleavage of aromatic bicyclic alkoxy radicals. *Chem. Phys. Lett.* **2006**, *432*, 313–320.
47. Fan, J.; Zhao, J.; Zhang, R. Theoretical study of OH addition to α - and β -pinenes. *Chem. Phys. Lett.* **2005**, *411*, 1–7.
48. Zhang, D.; Zhang, R. Ozonolysis mechanisms of α - and β -pinenes: Kinetics and mechanism. *J. Chem. Phys.* **2005**, *122*, 1–12.
49. Suh, I.; Zhang, R.; Molina, L.T.; Molina, M.J. Oxidation mechanism of aromatic peroxy and bicyclic radicals from OH-toluene reactions. *J. Am. Chem. Soc.* **2003**, *125*, 12655–12665.
50. Zhang, D.; Zhang, R.; Park, J.; North, S.W. Hydroxyperoxy nitrites and nitrates from OH initiated reactions of isoprene. *J. Am. Chem. Soc.* **2002**, *124*, 9600–9605.
51. Jiang, L.; Wang, W.; Xu, Y. *Ab initio* investigation of O₃ addition to double bonds of limonene. *Chem. Phys.* **2010**, *368*, 108–112.
52. Lei, W.; Derecskei-Kovacs, A.; Zhang, R. *Ab initio* study of OH addition reaction to isoprene. *J. Chem. Phys.* **2000**, *113*, 5354–5360.
53. Zhang, D.; Zhang, R. Mechanism of OH formation from ozonolysis of isoprene: A quantum-chemical study. *J. Am. Chem. Soc.* **2002**, *124*, 2692–2703.
54. Fukui, K. The path of chemical reactions—the IRC approach. *Acc. Chem. Res.* **1981**, *14*, 363–368.
55. Qu, X.; Wang, H.; Zhang, Q.; Shi, X.; Xu, F.; Wang, W. Mechanistic and kinetic studies on the homogeneous gas-phase formation of PCDD/Fs from 2, 4, 5-trichlorophenol. *Environ. Sci. Technol.* **2009**, *43*, 4068–4075.
56. Zhang, Q.; Li, S.; Qu, X.; Shi, X.; Wang, W. A quantum mechanical study on the formation of PCDD/Fs from 2-chlorophenol as precursor. *Environ. Sci. Technol.* **2008**, *42*, 7301–7308.
57. Corchado, J.C.; Chuang, Y.-Y.; Fast, P.L.; Hu, W.; Liu, Y.; Lynch, G.; Nguyen, K.; Jackels, C.; Ramos, A.F.; Ellingson, B. *POLYRATE*, version 9.7; Computer Program for the Calculation of Chemical Reaction Rates for Polyatomics; University of Minnesota: Minneapolis, MN, USA, 2007.
58. National Institute for Standards and Technology (NIST), 2008, Chemical Kinetics Database on the Web, Standard Reference Database 17. Available online: <http://kinetics.nist.gov/kinetics/Detail?id=1997DEM/SAN1-266:385> (accessed on 17 November 2014).